ULTRASOUND IMAGE RECONSTRUCTION FROM COMPRESSED MEASUREMENTS USING APPROXIMATE MESSAGE PASSING

J-H. Kim[1]*, A. Basarab*[2]*, P.R. Hill*[1]*, D.R. Bull*[1]*, D. Kouamé*[2]*, and A. Achim*[1]

[1]Visual Information Laboratory, University of Bristol,
Bristol, BS8 1UB, UK e-mail: (alin.achim@bristol.ac.uk)
[2]IRIT UMR CNRS 5505, University of Toulouse, CNRS, INPT, UPS, UT1C, UT2J, France

ABSTRACT

In this paper we propose a novel framework for compressive sampling reconstruction of biomedical ultrasonic images based on the Approximate Message Passing (AMP) algorithm. AMP is an iterative algorithm that performs image reconstruction through image denoising within a compressive sampling framework. In this work, our aim is to evaluate the merits of several combinations of a denoiser and a transform domain, which are the two main factors that determine the recovery performance. In particular, we investigate reconstruction performance in the spatial, DCT, and wavelet domains. We compare the results with existing reconstruction algorithms already used in ultrasound imaging and quantify the performance improvement.

Index Terms— ultrasonic images, Compressive Sampling, nonconvex optimization, IRLS, AMP, image denoising

1. INTRODUCTION

Ultrasonography is a highly attractive medical imaging modality that does not require any ionizing radiation or exposure of the patient to artificial electromagnetic fields. The new demands such as telemedicine applications and real time 3D imaging inevitably entail a significantly increased amount of data and/or longer acquisition time under the contemporary ADC architecture based on Nyquist sampling theorem, that argues that a band-limited analog signal can be perfectly recovered as long as the sampling rate is at least twice higher than its maximum frequency.

In 2006, Donoho [1] and Candes *et al.*[2, 3] introduced a novel theory called Compressed Sensing or Compressive Sampling (CS), giving theoretical proofs that sampling even below the Nyquist rate can lead to accurate reconstruction by exploiting signals sparsity or compressibility. Compressive sensing is based on measuring a significantly reduced number of samples than what is dictated by the Nyquist theorem. This has also potential benefits in ultrasound imaging since it can facilitate reduced storage space and transmission bandwidth due to the inherent compression achieved. With the advent of new technologies in signal processing, the challenges that ultrasound (US) imaging is currently facing, are expected to be overcome by CS framework. The objective of this paper is to propose enhanced CS recovery algorithms for compressively sampled US images, compared to previously proposed algorithms. The proposed method is based on the Approximate Message Passing (AMP) algorithm, a CS recovery technique that turns the reconstruction problem into an iterative denoising approach [4–6]. This paper focusses on the selection of a relevant sparsifying basis and a robust denoiser in order to maximize the performance of AMP in ultrasound CS reconstruction. The rest of the manuscript is organized as follows. In the following section, we provide a brief overview of CS and of the AMP algorithm. Section slowromancapiii@ introduces the proposed AMP-based reconstruction method adapted to US images. Experimental results are reported in Section slowromancapiv@, which also describes the methodology employed for simulations. Finally, section slowromancapv@ is devoted for the summary, main conclusion, and future work directions.

2. BACKGROUND

2.1. Compressive Sampling model

Introduced in [1–3], CS proposes theoretical guarantees for "perfect" recovery of an N-sample signal, having a K-sparse representation in a given basis, from M linear measurements, with $K < M \ll N$. The direct CS model is as follows:

$$y = \Theta x = \Phi\Psi\alpha \tag{1}$$

where x is a $N \times 1$ discrete signal, α is a $N \times 1$ signal having K non-zero elements and y is an $M \times 1$ vector containing the compressed measurements. Θ of size $M \times N$ is the measurement matrix, written as the product between a random matrix Φ (e.g., formed by M Gaussian [7] or Bernoulli [8] vectors with N samples) and Ψ that represents the $N \times N$ sparsifying transform (e.g. the transforms usually used in image compression). CS framework states that α can be recovered from the measurements y through the non linear optimization process in (2), provided that the measurement matrix Θ respects

978-0-9928-6265-7/16/$31.00 ©2016 IEEE

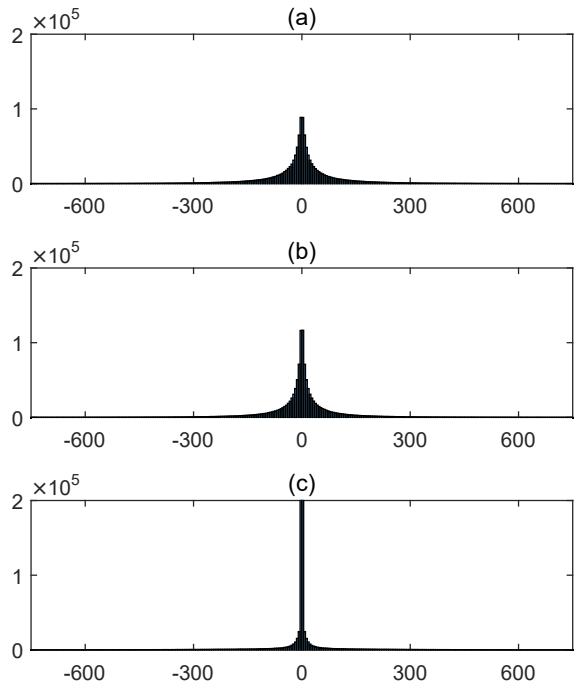

Fig. 1: Coefficient distribution of a standard ultrasound image in: (a) space, (b) wavelet and (c) DCT domains.
Horizontal and vertical axes represent the data and the number of sample, respectively.

the restricted isometry property [9]. In other words, this property imposes that the sampling vectors (the rows of Φ) should be as little correlated as possible to the vectors forming the sparsifying matrix Ψ.

$$\hat{\alpha} = \min_{\alpha} \|\alpha\|_1 \qquad \text{subject to} \qquad \Phi\Psi\alpha = y \tag{2}$$

2.2. Basics of approximate message passing

Inspired by belief propagation techniques, the approximate message passing (AMP) algorithm has been introduced in [4] as an alternative to CS reconstruction techniques that are based on minimizing (2) or similar objective functions. At each iteration, AMP consists of two steps as shown in equations (3) and (4).

$$x^{t+1} = \eta_t(\Theta^* z^t + x^t) \tag{3}$$

$$z^t = y - \Theta x^t + \frac{1}{\delta} z^{t-1} \langle \eta_{t-1}^{'}(\Theta^* z^{t-1} + x^{t-1}) \rangle \tag{4}$$

Here, the superscript 't' indicates iteration index and x^t is the estimate of x at t^{-th} iteration. $\eta_t(\cdot)$ is component-wise shrinkage/thresholding function whose derivative is denoted by $\eta_t^{'}(\cdot)$. Θ^* corresponds to the transpose of measurement matrix Θ. Finally, z^t of size $M \times 1$, δ, and $\langle \cdot \rangle$ represent the current residual (error), measurement rate M/N, and $\langle x \rangle = \frac{1}{N} \sum_{i=1}^{N} (x_i)$, respectively. The particularity that clearly differentiates AMP from existing iterative thresholding algorithms consists in the last term of the right hand side of (4), called Onsager reaction term in statistical physics and derived from the theory of belief propagation. Its contribution to improving the tradeoff between sparsity and undersampling rate has been shown in [4]. Initially proposed for signal reconstruction, AMP has been extended to images in [10], by performing the denoising in the wavelet domain.

3. AMP-BASED ULTRASOUND IMAGE RECONSTRUCTION

In this section we introduce an AMP-based ultrasound reconstruction algorithm capable of recovering the image from compressed measurements. To do so, two crucial points are evaluated in this paper: the sparsity of ultrasound images and the denoising method embedded in the AMP algorithm. Sparsity has a crucial effect on the measurement rate (M/N) needed and hence, reconstruction performance. Therefore it is crucial for improving recovery accuracy to find a transform able to sparsely represent the data through image coefficients. In the literature related to CS in US imaging, several transforms have been employed, ranging from standard wavelet or Fourier transforms to dictionary learning [11]. Figure 1 compares the ability for sparse representation of a standard US RF image in three different domains.
According to Figure 1, it is obvious that DCT coefficients exhibit far heavier tailed distribution than their other counterparts. Consequently, it is expected that the recovery performance of DCT outperforms its counterparts while using AMP with the same denoiser. In the following, the DCT will be denoted by the $N \times N$ matrix D, playing the role of Ψ in (1). In this research, two types of denoisers, serving as $\eta_t(\cdot)$ function in equations (3) and (4), are inbuilt in the AMP algorithm: the standard Soft Thresholding (ST) and Amplitude-scale-invariant Bayes Estimator (ABE) [12]. The analytical expressions of the two denoisers employed and of their derivatives are given hereafter.

ST denoiser:

$$\eta(x) = sign(x)(|x| - T)\mathbb{I}_{(|x|>T)}$$
$$\eta^{'}(x) = \mathbb{I}_{(|x|>T)} \tag{5}$$

where T is a threshold automatically calculated at each iteration following [13].

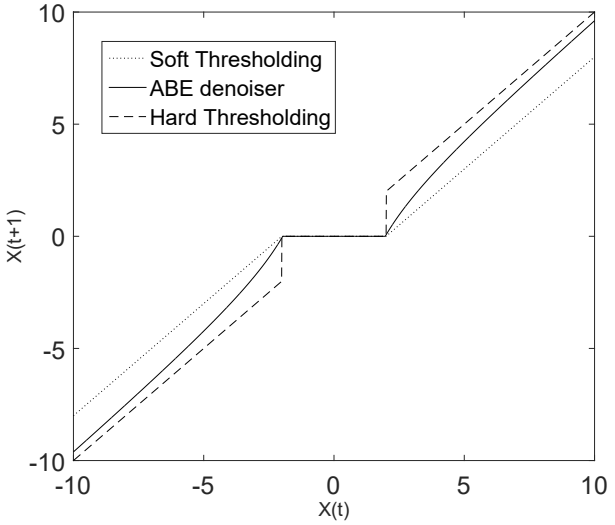

Fig. 2: Behavior of ABE and ST denoisers compared to the hard thresholding.

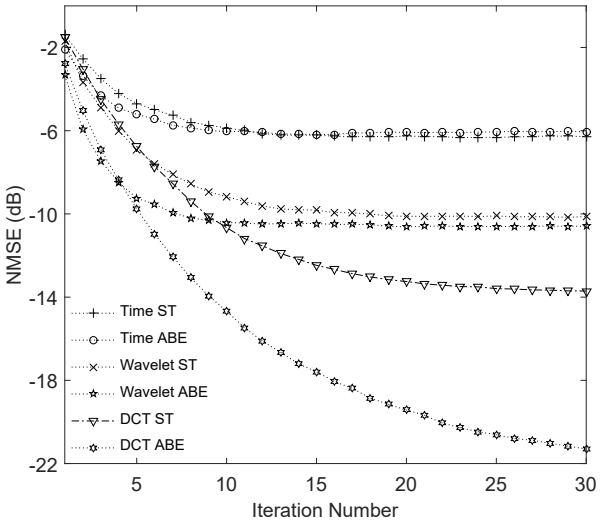

Fig. 3: Normalised Mean Squared Error (NMSE) vs iteration number.

ABE denoiser:

$$\eta(x) = \frac{(x^2 - 3\sigma^2)_+}{x}$$
$$\eta^{'}(x) = \mathbb{I}_{(x^2>3\sigma^2)}\big(1 + 3(\frac{\sigma}{x})^2\big) \quad (6)$$

where σ^2 is the noise variance, estimated at each iteration as a function of the current residual: $\sigma^2 = \frac{1}{M}\sum_{i=1}^{M}(z_i)^2$. The difference between the two denoisers employed may be observed in Figure 2.

The AMP algorithm summarized in (3) and (4), when modified to exploit the sparsity of US images in the DCT domain, becomes:

$$\theta_x^{t+1} = \eta_t\Big((\Theta D^{-1})^* z^t + \theta_x^*\Big) \quad (7)$$

$$z^t = y - (\Theta D^{-1})\theta_x^t + \frac{1}{\delta} z^{t-1}\big\langle \eta_{t-1}^{'}(\Theta D^{-1})^* z^{t-1} + \theta_x^{t-1})\big\rangle$$
$$= y - \Theta x^t + \frac{1}{\delta} z^{t-1}\big\langle \eta_{t-1}^{'}(\Theta D^{-1})^* z^{t-1} + \theta_x^{t-1})\big\rangle \quad (8)$$

where θ_x^t is the DCT transform of the US image x^t at iteration t, $i.e.$ $\theta_x^t = Dx^t$. In (11), $(\Theta D^{-1})^*$ is rewritten simply $D\Phi^*$ due to orthogonality of $D, i.e.$ $DD^* = I$. As a result, the input data of the denoising $\eta_t(\cdot)$ function is $D\Theta^* z^t + \theta_x^t$. The implementation of the proposed iterative algorithm summarized in (7) and (8) is based on [10]. The initialization consists in setting x^t to a zero-vector, and subsequently calculate z^t, $i.e.$ residual term. From these outcomes, the noisy measurement $\Theta^* z^t + x^t$ is computed and further transformed in the DCT domain by multiplying by D. The resulting vector serves as the input data for the shrinkage function, $\eta_t(\cdot)$ in (7). Furthermore, the denoised coefficients θ_x^{t+1} are obtained through denoising using $\eta_t(\cdot)$. Finally, we perform the inverse DCT transform by multiplying by D^{-1} in order to obtain the current estimate, x^{t+1}, which is utilized to calculate again the residual term z^{t+1} in (8). These process iterate until a reasonable stopping criterion is satisfied.

4. SIMULATION RESULT

Table 1: Quantitative results for the reconstructed images with the different evaluated techniques.

METHODS	DOMAIN	DENOISER	PSNR(dB)	SSIM
IRLS	DCT	-	16.31	0.66
AMP	TIME	SoftThreshold	9.09	0.14
		ABE	8.57	0.09
	WAVELET	SoftThreshold	12.46	0.28
		ABE	12.38	0.25
	DCT	SoftThreshold	18.56	0.54
		ABE	28.82	0.80
BM3D-AMP	BM3D	3D-Transform	23.95	0.86

4.1. Comparative methods

Two methods were used as benchmark to evaluate the performance of the proposed AMP-based US image reconstruction from compressed measurements. The first one is similar to (2), but uses a more general l_p optimization problem solved with the iteratively reweighted least squares (IRLS) algorithm

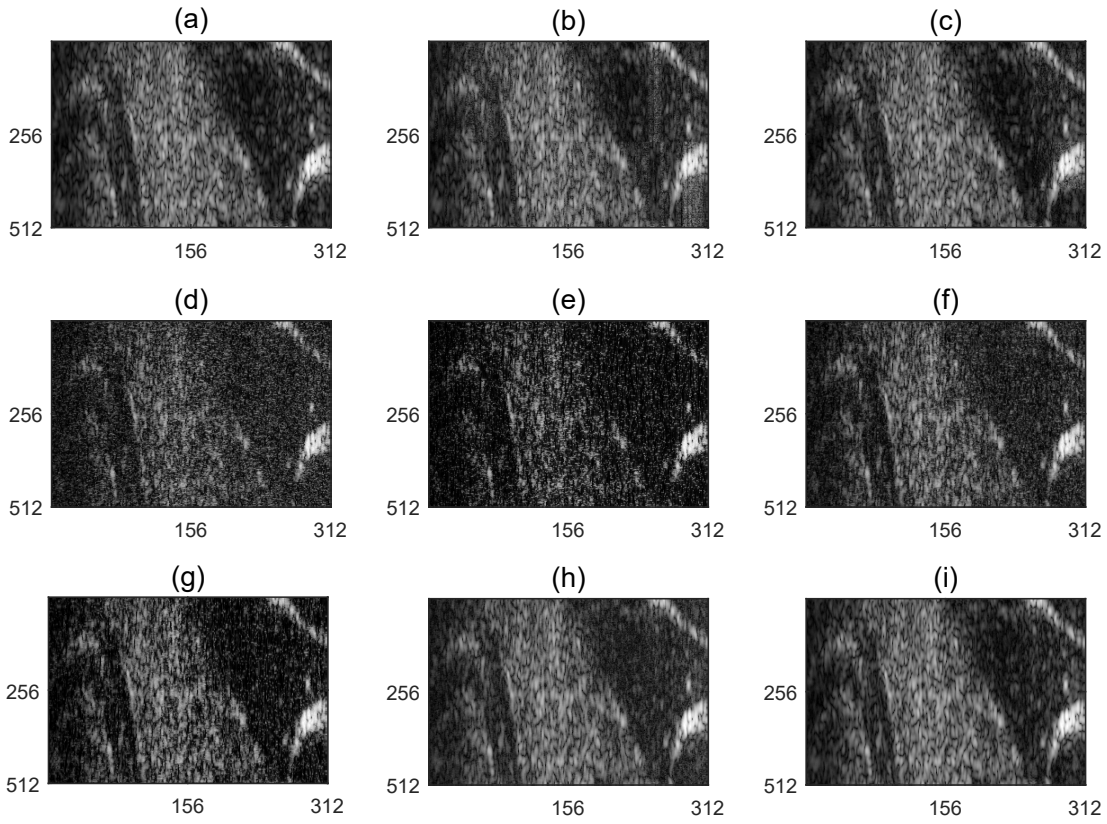

Fig. 4: (a) Original US RF image, Reconstructed images with (b) IRLS, (c) D-AMP, AMP-based algorithm (d)-(e) in image domain with ST and ABE denoiser, (f)-(g) in wavelet domain with ST and ABE denoiser, (h)-(i) in DCT domain with ST and ABE denoiser.

[13]. Based on the assumption that US signals follow an α-stable distribution [14, 15], the method in [16] uses the characteristic exponent α , calculated by fitting an α-stable distribution to the DCT of US images, to estimate an optimal value of p required for l_p optimization, $i.e.$ $p = \alpha - 0.01$. This way of choosing p has been shown to lead to better US reconstruction performance compared to standard basis pursuit and orthogonal matching algorithms [16, 17].

D-AMP equipped with BM3D as a denoiser, shown in [18] to enhance CS reconstruction performance even for nonsparse images, was the second method used for comparison. Several configurations of the proposed AMP-based reconstruction method in US imaging have been tested, by combining three domains (spatial, wavelet, and DCT) and two denoisers (ST and ABE). The wavelet transform was implemented using the Symmlet filter with four vanishing moments.

4.2. Reconstruction results

IRLS [13, 16], D-AMP [18] and the proposed AMP-based reconstruction algorithm using six combinations of image representations and denoisers are evaluated on an US image acquired with a clinical scanner (Sonoline Elegra) that was modified for research and a 7.5-MHz linear probe (Siemens Medical Systems, Issaquah, WA, USA), giving access to RF data sampled at 50 MHz. Also, the algorithms were implemented on HP ENVY running a 2.6GHz Intel(R) CoreTM i7-6500C processor with 8GB RAM under the Matlab R2014a environment. The image was cropped to 512 samples per 312 RF lines. The CS measurements have been generated by projecting this image onto an $M\mathbf{x}N$ matrix whose columns were $\mathcal{N}(0, \frac{1}{M})$ distributed (hence each column vector of the matrix has unit l_2-$norm$). The measurement rate was fixed at 40% $(M/N = 0.4)$ throughout simulations. The results are evaluated using the following quantitative metrics: peak-signal-to-noise ratio (PSNR) and structure similarity (SSIM), as well as by visual inspection of the reconstructed images.

Table 1 shows the numerical results and Figure 3 illustrates the evolution of normalized mean squared error (NMSE) over six different methods. In Figure 4, the visual inspection for the eight compared reconstructed images $(b) \sim (i)$ leads us to the conclusion that the image reconstructed by AMP with ABE denoiser based on DCT domain was the closest to the original image.
By contrast, AMP applied in the image domain produced severely degraded images, because of the lack of sparsity. Table 1 provides the overall outcomes for the quantitative analysis for recovery performance, showing the superiority of DCT-based AMP framework with ABE denoiser.

5. CONCLUSIONS

The purpose of this paper was to show the interest of using AMP-based CS reconstruction techniques in ultrasound imaging. Given the sparsity of US data in the DCT domain, the proposed AMP framework performed the denoising step in this domain. Two different existing denoisers have been evaluated: the soft thresholding and the amplitude-scale-invariant Bayes estimator. The results have proven the superiority of the latter in our application. The AMP framework has also been shown to be superior to an existing US image reconstruction framework which minimizes the l_p using IRLS algorithm.

6. ACKNOWLEDGMENT

This work was supported in part by the Wellcome Trust Institutional Strategic Support Fund through the Elizabeth Blackwell Institute at the University of Bristol.

7. REFERENCES

[1] D. Donoho, "Compressed sensing," Information Theory, IEEE Transactions on, vol. 52, pp. 1289-1306, April 2006.

[2] E. J. Candes, J. Romberg, and T. Tao, "Stable signal recovery from incomplete and inaccurate measurements," Communications on Pure and Applied Mathematics, vol. 59, no. 8, pp. 1207-1223, 2006.

[3] E. Candes, J. Romberg, and T. Tao, "Robust uncertainty principles: exact signal reconstruction from highly incomplete frequency information," Information Theory, IEEE Transactions on, vol. 52, pp. 489-509, Feb. 2006.

[4] D. L. Donoho, A. Maleki, and A. Montanari, "Message passing algorithms for compressed sensing," Proc. Nat. Academy Sci., vol. 106, no. 45, pp. 18914-18919, Nov. 2009.

[5] C. A. Metzler, A. Maleki, and R. G. Baraniuk, "From Denoising to compressed Sensing," Departments of Electrical and Computer Engineering, Rice University, Jul. 2014.

[6] Baek, H., Kang, J., Kim, K. and Lee, H., "Introduction and Performance Analysis of Approximate Message Passing (AMP) for Compressed Sensing Signal Recovery," The Journal of Korea Information and Communications Society, 38C (8), pp. 1029-1043, Nov. 2013.

[7] Z. Chen and J. Dongarra, "Condition numbers of Gaussian random matrices," SIAM Journal on Matrix Analysis and Applications, vol. 27, no. 3, pp. 603-620, 2006.

[8] E. Candes and T. Tao, "Near-optimal signal recovery from random projections: Universal encoding strategies," IEEE transactions on information theory, vol. 52, no. 12, pp. 5406-5425, 2006.

[9] E. Candes, "The restricted isometry property and its implications for compressed sensing," Comptes Rendus Mathematique, vol. 346, no. 9-10, pp. 589-592, 2008.

[10] Tan, J., Ma, Y. and Baron, D., "Compressive Imaging via Approximate Message Passing With Image Denoisin," IEEE Transactions on Signal Processing, 63(6), pp. 2085-2092, Feb. 2015.

[11] O. Lorintiu, H. Liebgott, M. Alessandrini, O. Bernard, and D. Friboulet, "Compressed sensing reconstruction of 3D ultrasound data using dictionary learning and line-wise subsampling," IEEE Transactions on Medical Imaging, vol. 34, no. 12, pp. 2467-2477, 2015.

[12] M. Figueiredo and R. Nowak, "Wavelet-based image estimation: An empirical Bayes approach using Jeffreys noninformative prior," IEEE Trans. Image Process., vol. 10, no. 9, pp. 1322-1331, Sept. 2001.

[13] R. Chartrand, W. Yin, "Iteratively reweighted algorithms for compressive sensing," IEEE International Conference on Acoustics, Speech and Signal Processing (ICASSP), pp. 3869-3872, 2008.

[14] M. A. Kutay, A. P. Petropulu, and C. W. Piccoli, "On modeling biomedical ultrasound RF echoes using a power-law shot noise model," IEEE Trans. Ultrason. Ferroelectr. Freq. Control, vol. 48, no. 4, pp. 953-968, Jul. 2001.

[15] Achim, A., Bezerianos, A. and Tsakalides, P., "Novel Bayesian multiscale method for speckle removal in medical ultrasound images," IEEE Transactions on Medical Imaging, 20(8), pp. 772-783, 2001.

[16] Achim, A., Basarab, A., Tzagkarakis, G., Tsakalides, P., Kouame, D., "Reconstruction of Ultrasound RF Echoes Modeled as Stable Random Variables," IEEE Trans. Comput. Imaging, 1(2), pp. 86-95, Jun. 2015.

[17] Achim, A., Benjamin Buxton, George Tzagkarakis, and Panagiotis Tsakalides, "Compressive Sensing for Ultrasound RF Echoes Using - Stable Distribution," in 32nd Annual International Conference of the IEEE EMBS (EMBC-2010), Buenos Aires, Argentina, pp. 4304-4307, 2010.

[18] C. A. Metzler, A. Maleki, and R. G. Baraniuk, "BM3D-AMP: A new image recovery algorithm based on BM3D denoising," IEEE International Conference on Image Processing, pp. 3116-3120, 2015.